13

Adhesion Forces Reduction by Oscillation and Its Application to Micro Manipulation

Tetsuyou Watanabe† and ZhongWei Jiang‡
†*Kanazawa University, Japan*
‡*Yamaguchi University, Japan*

1. Introduction

In a micro range, it is a key issue how to cope with adhesion which arises between an object and tools (see Fig. 1). To resolve the problem, many methods have been developed, including the adhesion-type micro end-effector (Arai et al., 1996 a) (Arai et al., 1996 b), the vacuum gripping tool (Zesch et al., 1997), releasing by slopping and oscillating an end-effector (Rollot et al., 2002) (Haliyo et al., 2002) (Haliyo et al., 2003), releasing by control of electrostatic force (Saito et al. 2003), and releasing strategy based on environment information (Saito et al., 2001). However, there are still unresolved problems such as the difficulty of object motion control after the release, the difficulty of practical execution of the method (Saito et al., 2001) (since it is almost impossible to acquire all required information).

In this chapter, we propose a new strategy to cope with adhesion forces and develop an automatic micro manipulation system. By minutely oscillating an end-effector, bringing it near to an object on a substrate (table) and contacting it with the object, the adhesion force between the end-effector and the object becomes small comparing with the adhesion force between the substrate (table) and the object (see Fig. 2). Then, it is easy to remove the end-effector from the object while the object adheres to the substrate. Hereafter, ***we call this (phenomenon) relaxation of adhesion force. If the object is removed from the end-effector at any time, we say the adhesion force is relaxed enough. If it is not and the object sometimes adheres to the end-effector, we say the adhesion force is not relaxed enough***. Using this strategy, it is expected to accurately manipulate micro object like macro manipulation.

But, this strategy is not always available. When the pushing force applied to the object by end-effector is large, the effect of oscillation decreases, and then the adhesion force is not reduced enough. Then, we propose a method to check the adhesion state; whether the adhesion force is relaxed enough or not. We measure the oscillation of the end-effector, and apply FFT to it. If the lower mode frequencies (than the frequency of the input oscillation) are excited, the adhesion force is reduced enough. Otherwise, the adhesion force is not reduced enough.

However, this method is available in only limited situations if using the laser displacement meter to measure the oscillation, because 1) the end-effector must be located at the specific

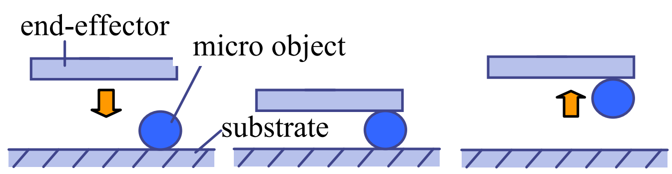

Fig. 1. Micro object adhered to end-effector

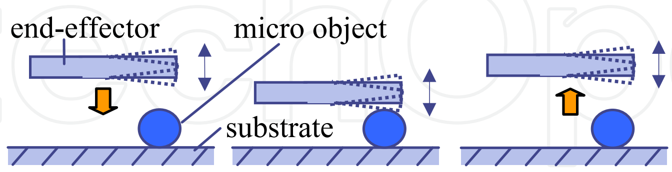

Fig. 2. Relaxation of adhesion force

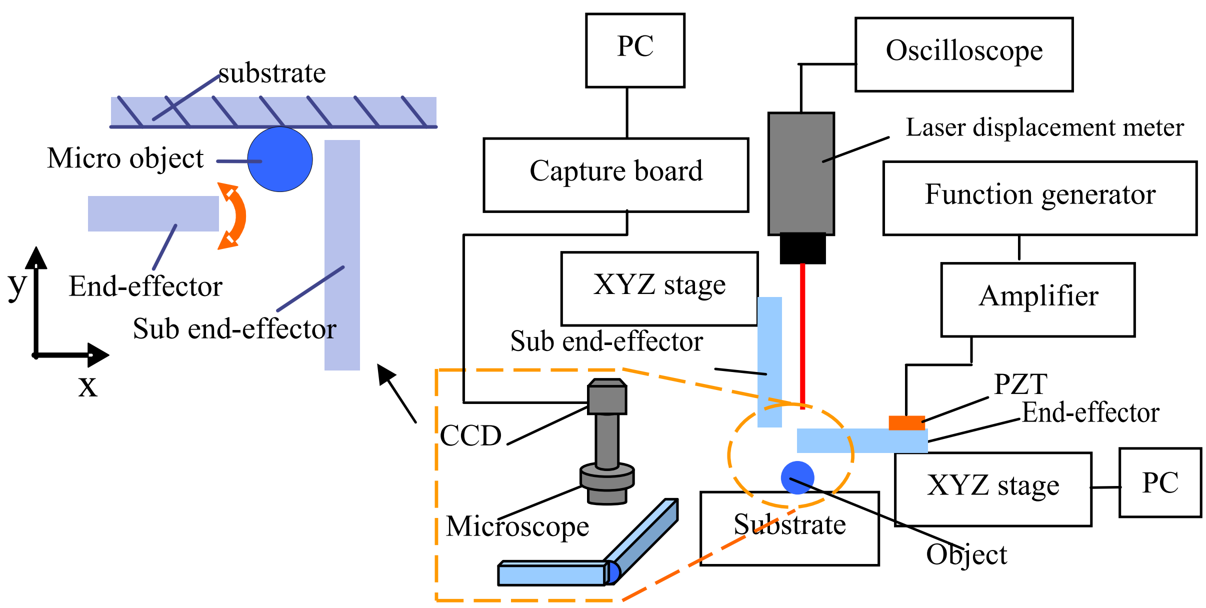

Fig. 3. Target system (Overview of experimental set up)

point where laser displacement meter can measure oscillation; 2) the adhesion state can not be checked if something blocks the light/laser or the target leaves the measuring point. So, it is hard to apply this method to micro manipulation directly. Then, we propose a method to check the adhesion state by vision. The oscillation of end-effector can not be perfectly caught by camera. Instead, the blur of the oscillation appears in the captured image. The amount of the blur is associated with the amplitude of the oscillation. Then, we develop a method to estimate the amplitude of oscillation by the blur. Subsequently, we focus that lower mode oscillation has large amplitude comparing with oscillation with higher mode frequency or no-resonance frequency. Utilizing this findings, we develop a method to detect lower mode frequencies by a blur. The adhesion state can be checked by checking whether lower mode frequencies are excited or not. Then, based on this findings and the method for detecting lower mode frequencies, we propose a method to check the adhesion state by vision. This method can be applied to any areas in the captured image and can be used all the time during manipulation. Its computational load is low. Since vision sensor is usually used in micro manipulation and any other sensors are not needed, the total system is very simple and low cost. Lastly, applying this method to micro manipulation, we develop an automatic control system for micro manipulation.

2. Target system

Fig. 3 shows the target system, which consists of manipulation part, image-capturing part, end-effector-oscillating part, and displacement-measuring part. For the simplicity, we assume that: (1) the manipulation is done in a planner space and a gravity force doesn't work, (2) the object is a sphere, (3) the end-effector, the sub end-effector and the substrate are made of a same material, (4) the end-effector, the sub end-effector and the substrate are grounded for preventing an extra charge at the initial state.

The manipulation part consists of end-effector, sub end-effector, micro object, and substrate. The end-effector and the sub end-effector are cantilever beams made of copper in size of 3x40x0.3[mm]. The beams are rolled copper, and any surface treatments such as grinding are not conducted. Young's modulus of copper is $1.02\mathrm{x}10^{11}$ [N/m^2], its Poisson's ratio is 0.35, and its density is 8900 [kg/m^3]. On the end-effector, the PZT (piezocell) (Fuji ceramics, Z0.2T50x50x50S-W C6) of 3x3x0.2 [mm] is bonded at the position of 1 [mm] from the clamped end for oscillating the end-effector. The surface of substrate is a copper cut bonded on an aluminum board. The end-effector and the sub end-effector are attached on XYZ stage (Surugaseiki, PMZG413) which can be controlled by PC. The object is a glass sphere (Union, unibeads) with a radius of 100 or 200 [10^{-6}m] and a copper sphere with a radius of 150 [10^{-6}m]. Young's modulus of glass is $7.05\mathrm{x}10^{10}$ [N/m^2], its Poisson's ratio is 0.17, and its density is 2500 [kg/m^3].

The image-capturing part consists of Video-microscope (Surugaseiki, VMU-V) with objective lens (Mitsutoyo S72M-5), CCD camera (Lumenera, LU135), and PC. The overview of the manipulation is captured by the CCD camera through the microscope and sent to PC. We use maximum illumination of light source (Schott MegaLight100-ROHS) whose maximum illumination is 24000[Lx] at the 100[mm] from the tip of the lighting system.

The end-effector is oscillated by oscillating the PZT by a function generator (NF, DF1906) through a power amplifier. The power amplifier is handmade circuit and its amplification ratio is set to 3.2.

The tip motion of the end-effector is measured by laser displacement meter (Sony VL10). The measured data is sent to PC through oscilloscope (Yokogawa DL1700).

3. Adhesion force relaxation and adhesion state estimation by laser displacement meter

By minutely oscillating the end-effector, bringing it near to an object on a substrate and contacting it with the object, the adhesion force between the end-effector and the object becomes small comparing with the adhesion force between the substrate and the object (see Fig. 2). This is thought to be mainly due to a hitting (impulse) effect and smaller time of

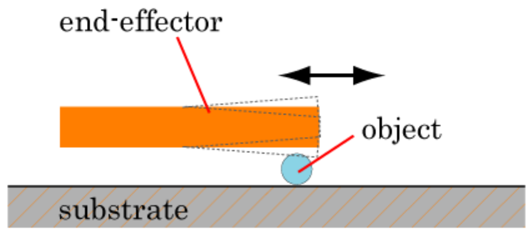

Fig. 4. Experiment to show adhesion force relaxation

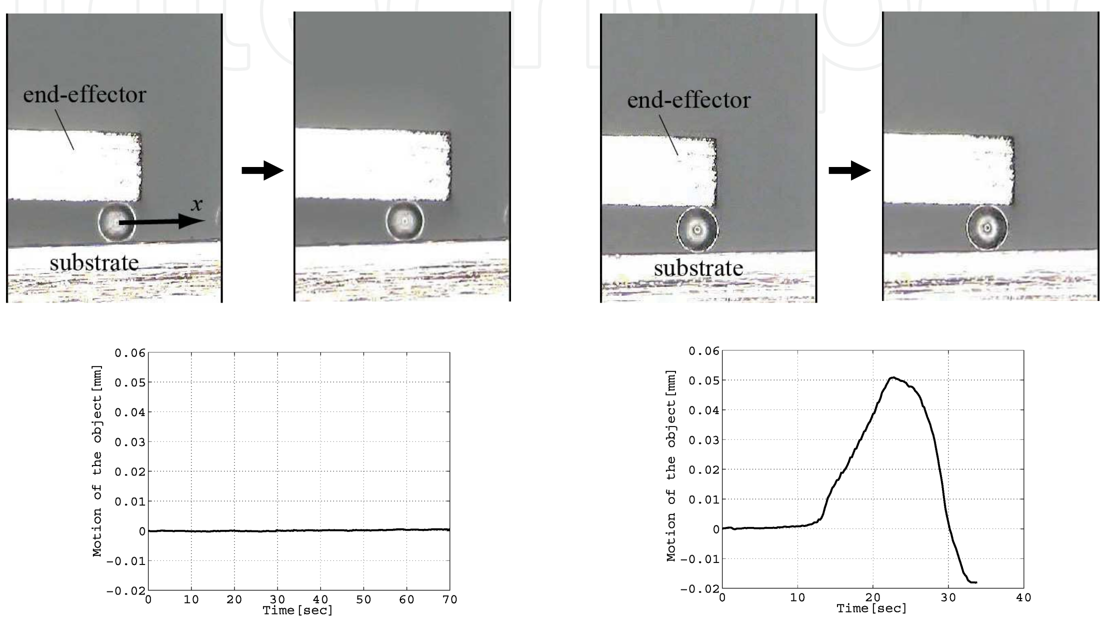

(a) when oscillating the end-effector

(b) when not oscillating the end-effector

Fig. 5. Overview of the experiment (upper figures) and the motion of the object center (lower figures)

contact between the object and the end-effector. Then, it is easy to remove the end-effector from the object while the object adheres to the substrate. Here we show simple experiment to show the effect as shown in Fig. 4. We bring the end-effector near to the object on the substrate, and contact it with the object. Subsequently, we move the end-effector in the left and right directions (of this page). We perform the experiments when the end-effector is oscillated and when it is not oscillated. We observe the motion of the object center. The object is a glass sphere. The input voltage to PZT is sine wave with the amplitude of 10[V]. Its frequency is 4th mode resonance frequency. Fig. 5 shows the result. The vertical axis denotes the position of the object center while horizontal axis denotes time. It can be seen that the end-effector slides on the object when oscillating the end-effector while the object rotates when not oscillating the end-effector. It means that end-effector oscillation can relax the adhesion force.

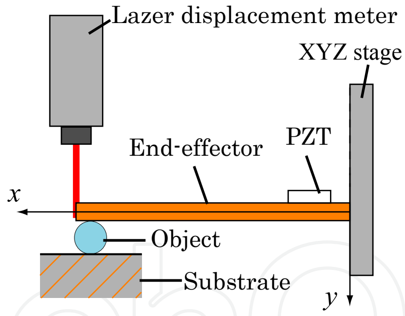

Fig. 6. Experimental set up for adhesion state check and its coordinate frame

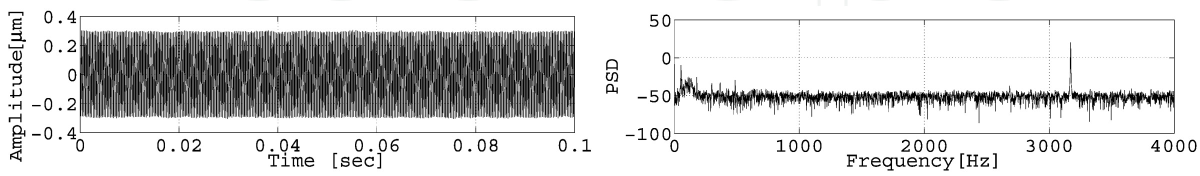

(a) $y_{x=0}$ = -3

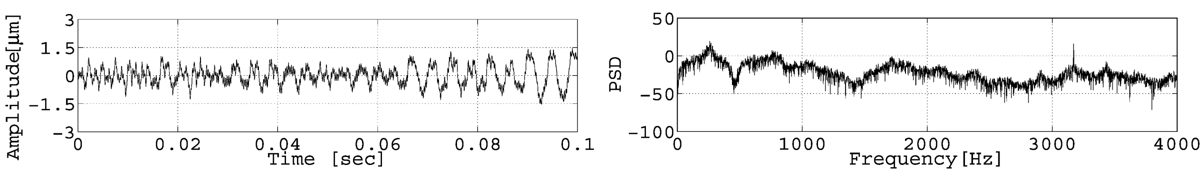

(b) $y_{x=0}$ = 3

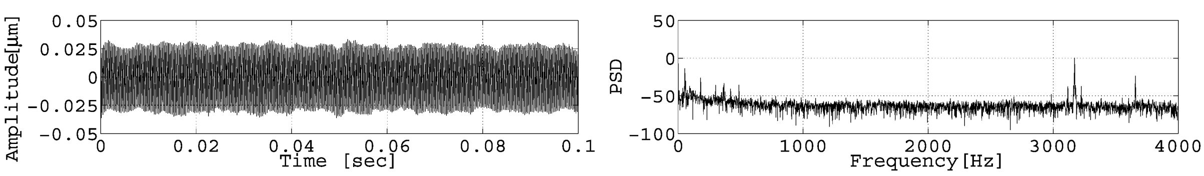

(c) $y_{x=0}$ = 8

Fig. 7. Tip displacement (left side) and power spectrum density (right side) when pushing the glass sphere by oscillated end-effector (5V)

3.1 adhesion state check by laser displacement meter

This method is not always available. If the pushing force applied to the object is large, oscillation effect decreases, and the adhesion force is not relaxed enough. Therefore, adhesion state has to be checked. Here, we propose a method for the check. Fig. 6 shows the experimental set up. We set y direction so that y can be orthogonal to the long side of the end-effector as shown in Fig. 6. We move the oscillated end-effector by moving the clamped end by XYZ stage, along y positive direction with the step of 1 [μm] from $y(x=0)=-3$ to y(x=0)=8 [μm]. Let y(x=0) when the end-effector firstly contacts with the object be 0. At the initial state (y(x=0)=-3), the end-effector does not contact with the object. At y(x=0)=0, the end-effector contacts with the object. At y(x=0)≥0, the end-effector pushes the object. y(x=0) corresponds to the magnitude of the pushing force. We measure the oscillation of the end-effector by the laser displacement meter. The input signal for the oscillation is sine curve whose amplitude is 5 [V], and whose frequency is 4th mode resonance frequency (this mode is selected so that enough large kinetic energy can be got while the amplitude can be small enough not to disturb the manipulation). The object is a

y[μm]	Frequency of adhesion / number of trial times
0～7	0/10
8	2/10

Table 1. Frequency of adhesion to the end-effector when removing the end-effector from the substrate.

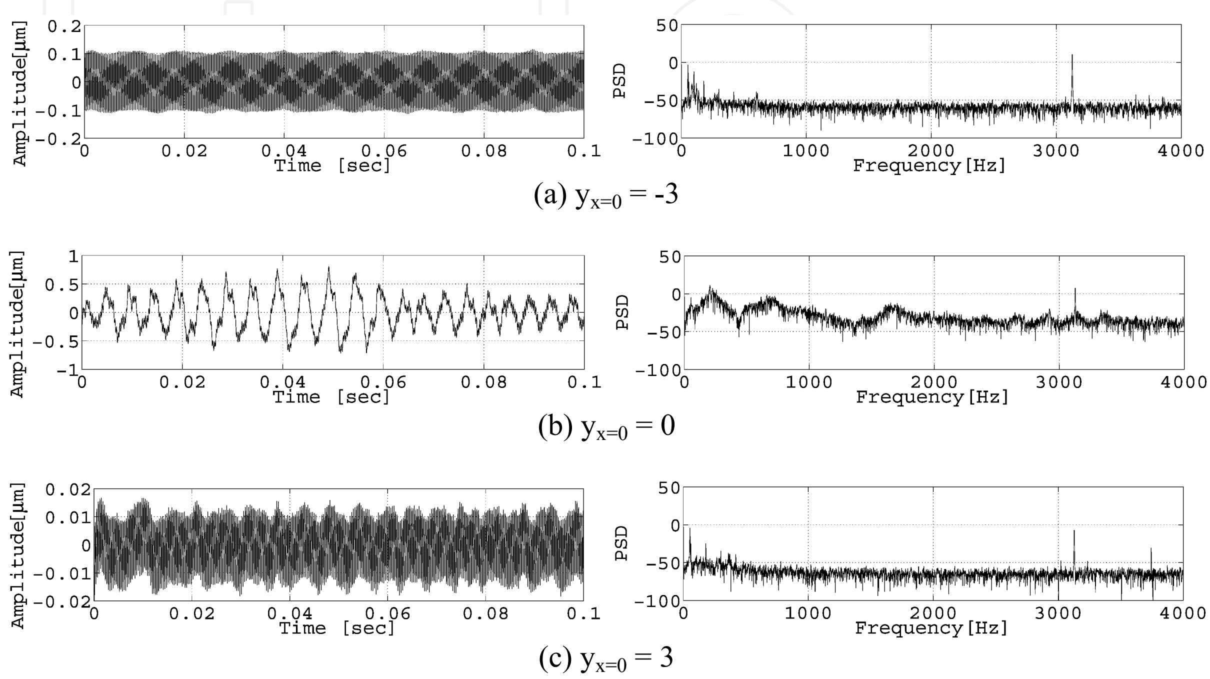

Fig. 8. Tip displacement (left side) and power spectrum density (right side) when pushing the glass sphere by oscillated end-effector (2.5V)

glass sphere with radius of 200 [μm]. The left figures of Fig. 7 show the tip displacement, and the right figures show the power spectrum density obtained by applying FFT to the measured tip displacement. The horizontal axis denotes time and the vertical axis denotes the amplitude at the left figures while the horizontal axis denotes the frequency and the vertical axis denotes the power spectrum density at the right figures. At y(x=0)=-3 [μm] (before contact), only inputted 4th mode frequency was observed as shown in Fig. 7 (a). At y(x=0)=0~7 [μm], the amplitude is larger than at y(x=0)=-3 [μm], and not only inputted 4th mode frequency but also lower mode frequencies were observed. Here, we show the case at y(x=0)=3 [μm] as a representative of the results (see Fig. 7 (b)). At y(x=0)=8 [μm], the amplitude is smaller than the other cases, and lower mode frequencies were not observed. At every case, we perform the experiment in which the end-effector is moved along y negative direction (removed from the substrate) 10 times. Table 1 shows the result. At y(x=0)=0~7 [μm], the object did not adhere to the end-effector at any time. Then, the adhesion force is thought to be relaxed enough. On the other hand, at y(x=0)=8 [μm], the object adhered to the end-effector twice. Then, the adhesion force is thought to be not relaxed enough due to smaller amplitude of the oscillation. It indicates that we can estimate whether adhesion force is relaxed enough or not by checking the excitation of the lower mode frequencies.

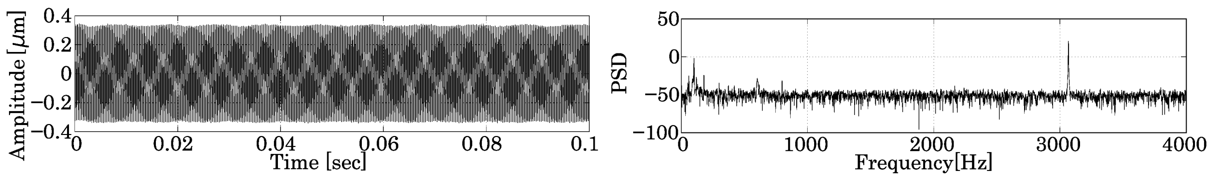

(a) $y_{x=0}$ = -3

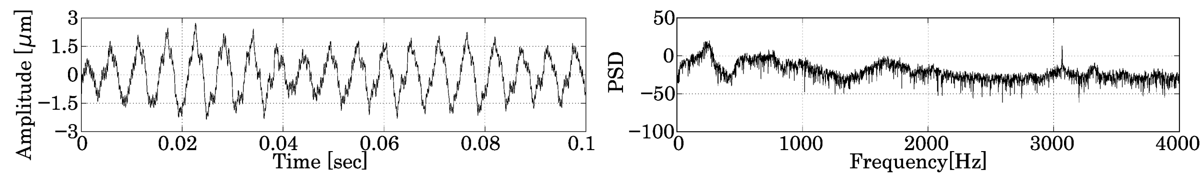

(b) $y_{x=0}$ = 1

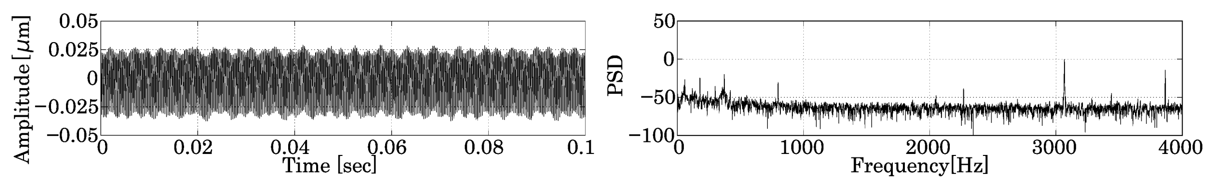

(c) $y_{x=0}$ = 6

Fig. 9. Tip displacement (left side) and power spectrum density (right side) when pushing the copper sphere by oscillated end-effector (5V)

Next, to investigate the effect of amplitude of input voltage to PZT, we change the amplitude from 5 [V] to 2.5 [V] and perform the same experiment. Fig. 8 shows the results. In addition, to investigate the effect of material of the object, we change the object from glass sphere to copper sphere with a radius of 150 [μm] and perform the same experiment. Fig. 9 shows the results. From Fig. 7, 8 and 9, it can be seen that our approach is available at any case. But, the amplitude of input voltage and the material of the object affect the available range of the proposed method (how much we can push the object, relaxing adhesion force). It can be seen that in order to get larger available range, the oscillation with larger energy (larger amplitude of input voltage) should be applied. Since surface energy of copper is 2 [J/m^2] while surface energy of glass is 0.08 [J/m^2] (Israelachvili, 1996), the adhesion force for copper sphere is larger than that for glass sphere. It is thought to be the reason why the available range for copper sphere is smaller than that for glass sphere.

4. Adhesion state estimation by vision

As mentioned the above, the proposed method to check adhesion state is available in only limited situations due to the use of laser displacement meter: 1) The end-effector must be located at the specific point where laser displacement meter can measure oscillation; 2) the adhesion state can not be checked if something blocks the light/laser or the target leaves the measuring point. So, it is hard to apply this method to micro manipulation directly. Concerning these problems, here we present a method to check the adhesion state by vision.

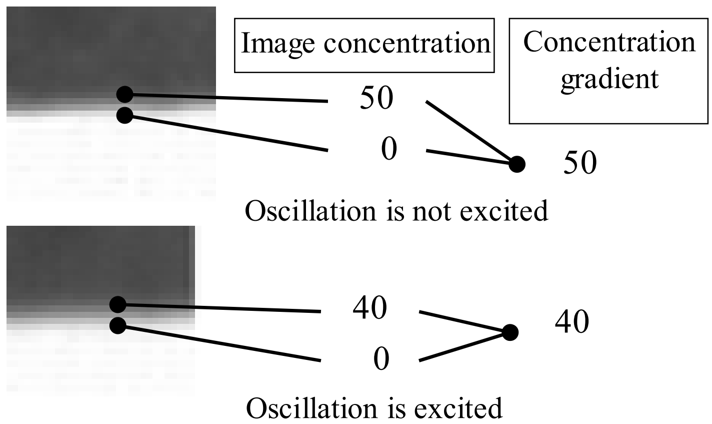

Fig. 10. Image concentration gradient

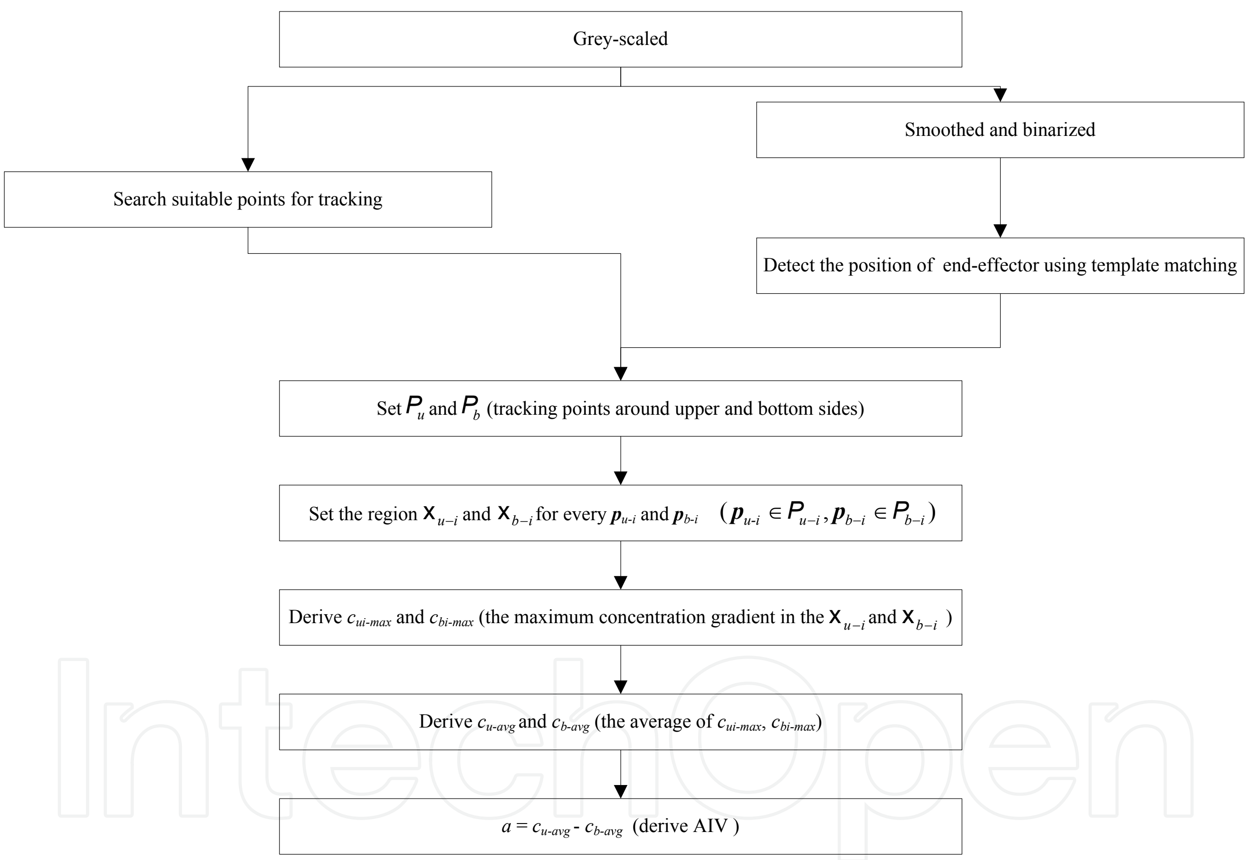

Fig. 11. Flowchart for deriving AIV (amplitude indicating value)

4.1 Oscillation amplitude estimation by vision

Firstly, we develop a method to estimate amplitude of oscillation using only vision information. Oscillation is too fast to be perfectly caught by camera. However, a blur resulted from the oscillation appears in the captured image. Then, we try to estimate the amplitude of the oscillation using the blur. When oscillation is not excited, the image concentration gradient (see Fig. 10) around the edge of the end-effector is large. On the other

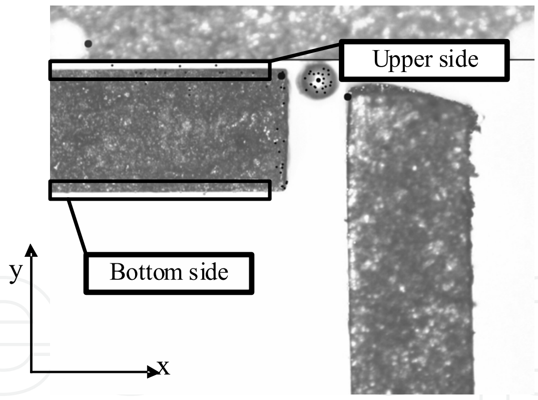

Fig. 12. Upper and bottom sides of the end-effector

hand, when oscillation is excited, it is small due to a blur. Using the concentration gradient, we estimate the amplitude of the oscillation. We call the estimated amplitude AIV (amplitude indicating value). The procedure for deriving AIV is shown in Fig. 11. First, the captured image is grey-scaled. Next, it is smoothed and binarized. Previously, we prepare the tip area image of the end-effector as a template image. By template matching technique which finds the part in the binarized image which matches the template image, we detect the position of end-effector. On the other hand, we search suitable points for tracking, ***p***, around the edge of the end-effector in the firstly grey-scaled image. Here, we pick up ***p'****s* located around the upper side (area of 10 pixel (about 10μm) from the upper edge), and let P_u be a set of the picked up points (see Fig. 12). Similarly, we pick up ***p'****s* located around the bottom side and let P_b be a set of the picked up points. Also, let $\boldsymbol{p}_{\mathbf{k\text{-}i}}$ be *i*th ***p*** contained in P_k ($k \in \{u,b\}$), let n be the number of $\boldsymbol{p}_{\mathbf{u\text{-}i}} \in P_u$, and let m be the number of $\boldsymbol{p}_{\mathbf{b\text{-}i}} \in P_b$. We calculate $l_{k\text{-}i}$ which is the length between $\boldsymbol{p}_{k\text{-}i}$ and its nearest side/edge. Then, we derive the maximum value of $l_{k\text{-}i}$:

$$l_{\max} = \max_{i,k} l_{k-i} \tag{1}$$

Using $l_{\max}$, we define the following region $X_{k\text{-}i}$ for $\boldsymbol{p}_{k\text{-}i}$:

$$X_{k-i} = \left\{ (x,y) \middle| \begin{matrix} p_{k\text{-}ix} - 0.6 * l_{max} \le x \le p_{k\text{-}ix} + 0.6 * l_{max} \\ p_{k\text{-}iy} - 1.4 * l_{max} \le y \le p_{k\text{-}iy} + 1.4 * l_{max} \end{matrix} \right\} \tag{2}$$

where $p_{k\text{-}ix}$ and $p_{k\text{-}iy}$ are, respectively, x and y components of $\boldsymbol{p}_{k\text{-}i}$. Here, 0.6 and 1.4 are set by trial and error so that the nearest side/edge can be contained in $X_{k\text{-}i}$ and the variation of the maximum image concentration gradient in the $X_{k\text{-}i}$ can be small. Let $c_{ki\text{-}max}$ be the maximum concentration gradient in the $X_{k\text{-}i}$. We compute $c_{ki\text{-}max}$ for every $\boldsymbol{p}_{k\text{-}i}$ ($X_{k\text{-}i}$) and derive its average value $c_{k\text{-}avg}$:

$$\begin{aligned} c_{u-avg} &= (\textstyle\sum_{i=1}^{n} c_{ui-\max})/n \\ c_{b-avg} &= (\textstyle\sum_{i=1}^{m} c_{bi-\max})/m \end{aligned} \tag{3}$$

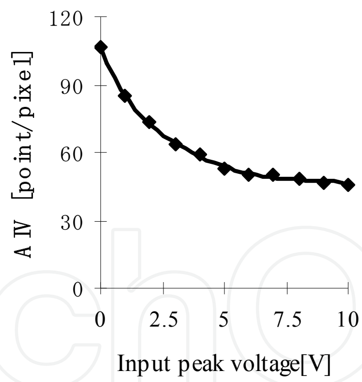

Fig. 13. Relation between the input peak voltage and AIV

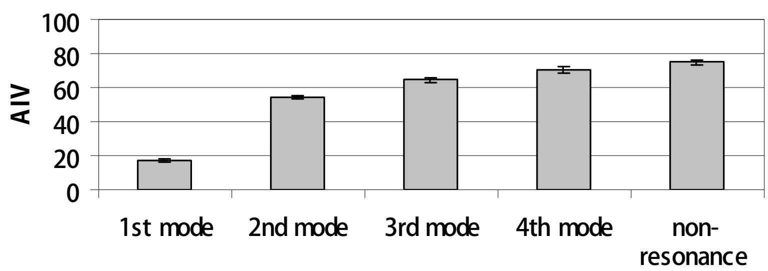

Fig. 14. AIV for several mode frequencies

From (3), we define the amplitude indicating value (AIV) a as follows:

$$a = C_{u-avg} - C_{b-avg} \tag{4}$$

Here, we confirm the efficiency of AIV by experiment. We oscillate the cantilevered end-effector freely. The input voltage for PZT is square wave whose peak to peak is from 0 to 0-10 [V], whose duty ratio is 50[%] , and whose frequency is 1st mode frequency 0.18[kHz]. AIV is computed by the program written by C++ language using OPEN CV library.

Fig. 13 shows the result. The horizontal axis expresses the input peak voltage, and the vertical axis expresses the computed AIV. Note that the input peak voltage indicates amplitude of oscillation since the voltage is proportional to the amplitude. By applying regression analysis, the relation is expressed by v=85$a^{-0.27}$ where v denotes the input peak voltage. From the result, it can be seen that the amplitude of oscillation can be estimated by AIV at 0≤v≤ 5 [V]. On the other hand, it is hard to estimate the amplitude at v ≥ 6 [V], although it can be detected that the oscillation has larger amplitude than a certain constant value (for example, the amplitude at v=5 [V]).

4.2 Discrimination between higher and lower mode frequencies by AIV

When bringing the oscillated end-effector with high mode frequency close to the object on the substrate and lower mode frequencies are excited, the adhesion force between the end-

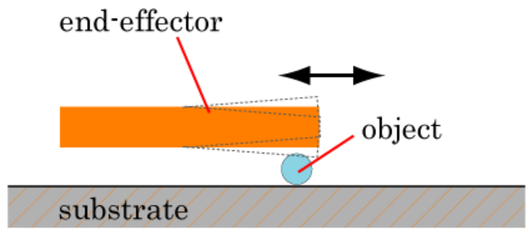

Fig. 15. Overview of the experiment for checking whether adhesion state can be estimated by AIV

effector and the object is reduced. Then, if discriminating between higher and lower mode frequencies by AIV, we can detect the adhesion state by AIV. Here, we investigate whether or not higher and lower mode frequencies can be discriminated by AIV by experiment.

We oscillate the cantilevered end-effector freely. The input voltage for PZT is square wave whose peak to peak is from 0 to 24 [V], whose duty ratio is 50[%], and whose frequency is 1st - 4th mode frequency. For the comparison, we also select non-resonance frequency of 2 [kHz].

Fig. 14 shows the results. From Fig. 14, it can be seen that the higher the frequency mode is, the larger AIV is. It is thought to come from that the higher frequency mode is, the smaller the amplitude is. The difference between AIV's for 1st mode and the other modes (including non-resonance frequency) is very large, and then the 1st mode oscillation can be easily detected. The 2nd mode oscillation can also be discriminated from the other higher mode oscillations by checking the difference of AIV. On the other hand, the discriminations between 3rd and 4th modes and between 4th mode and non-resonance frequencies are not easy. If setting the threshold for the discrimination is 3, we can discriminate 3rd and 4th modes frequencies, and 4th mode and non-resonance frequencies. If setting it is over 5, we can discriminate neither. In short, we can detect lower mode frequencies by AIV.

4.3 Detection of adhesion state by AIV

Base on the previous subsection results, we investigate whether adhesion state can be estimated by AIV.

We take the following way (see Fig. 15). First, we bring the oscillated end-effector close to the object and contact the end-effector with the object. Next, we move the end-effector in the left and right directions (of this page). If adhesion force is reduced enough, the end-effector slides on the object while the object is at stationary state. If it is not reduced enough, the object rotates. In the case when the end-effector slides on the object, we increase the pushing force applied to the object by moving the end-effector along y positive direction (refer to y direction in Fig. 6)…, and move the end-effector in the left and right directions again. This procedure is repeated until the object rotates. The input voltage for the oscillation is square wave whose peak to peak is from 0 to 24 [V], whose duty ratio is 50[%], and whose frequency is 4th mode frequency. The experience was done 5 times.
The results are shown in Fig. 16. Free means the end-effector is oscillated without contacting with the object. Note that in this experiment, the value of AIV when adhesion force is reduced enough changes with the change of the pushing force. Then, AIV in that case is

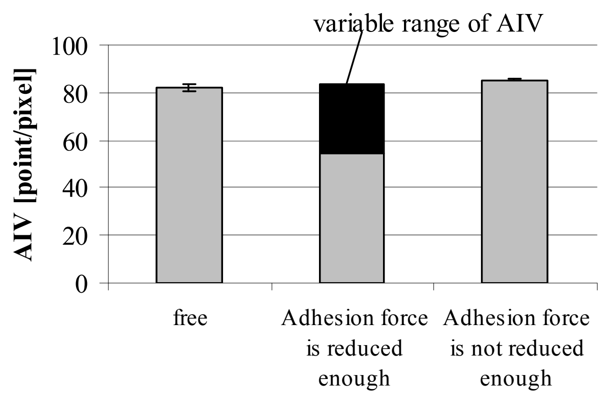

Fig. 16. AIV's when adhesion force is reduced enough and not reduced enough (AIV is shown by range because AIV when adhesion force is reduced enough changes with the change of the pushing force applied to the object)

shown by range. From Fig. 16, it can be seen that AIV when adhesion force is reduced enough is smaller than or equal to AIV for free state. The maximum difference is about 20. It is the reason why the lower mode frequencies (than the frequency of the inputted oscillation) are excited. On the other hand, AIV when adhesion force is not reduced enough is larger than AIV for free state. It is the reason why if the pushing force applied to the object is large, the energy of oscillation decreases and then the amplitude of the oscillation becomes smaller than that in the free state (refer to Fig. 7).

Note that AIV for 4th mode in Fig. 14 is different from AIV for free state in Fig. 16. It is due to the large difference of the end-effector position. The illumination or light intensity differs from place to place. Then, if the end-effector position changes largely, AIV also changes. Therefore, in order to check adhesion state, we use the difference between AIV when the end-effector is freely oscillated around the target point and AIV when the end-effector contacts with the object. Note also that there is the case when AIV when adhesion force is reduced enough is almost same as AIV for free state. It is thought that the lower mode frequencies are excited but their amplitude is small, and then AIV is large. In such a case, it is difficult to estimate adhesion state: whether adhesion force is reduced enough or not. However, a precious control of the pushing force applied to the object does not need in the target operation. Therefore, we only have to control the end-effector so that the difference between AIV's for free case and the case when the end-effector contacts with the object can be included in the appropriately defined range. Then, we can keep adhesion force reduced enough, while pushing the object with enough large force.

5. Automatic micro manipulation system

Using the developed method for estimating the adhesion state by vision, we develop a system which automatically pick and place a micro object. We use the experimental set up described at section 2 (see Fig. 3).

We present a procedure for picking operation in Fig. 17 (refer to the real movement shown in Fig. 19). First, using template matching technique, we find the tip positions of the end-

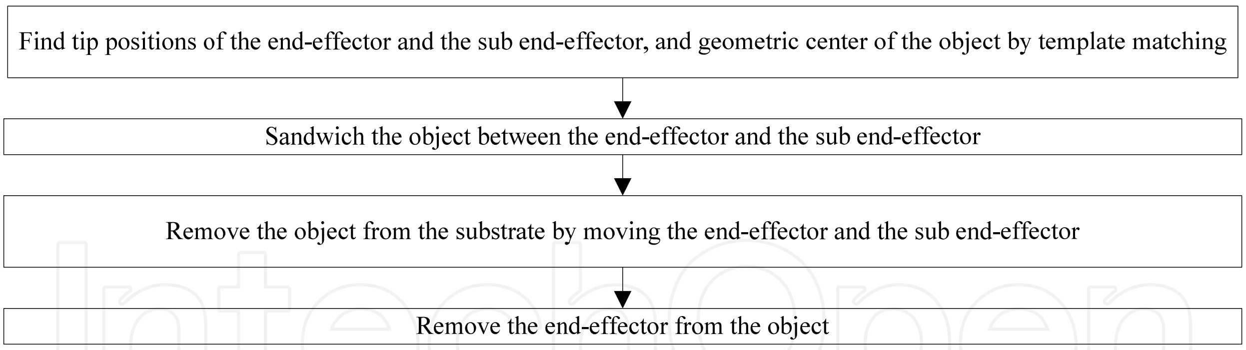

Fig. 17. Flowchart for picking operation

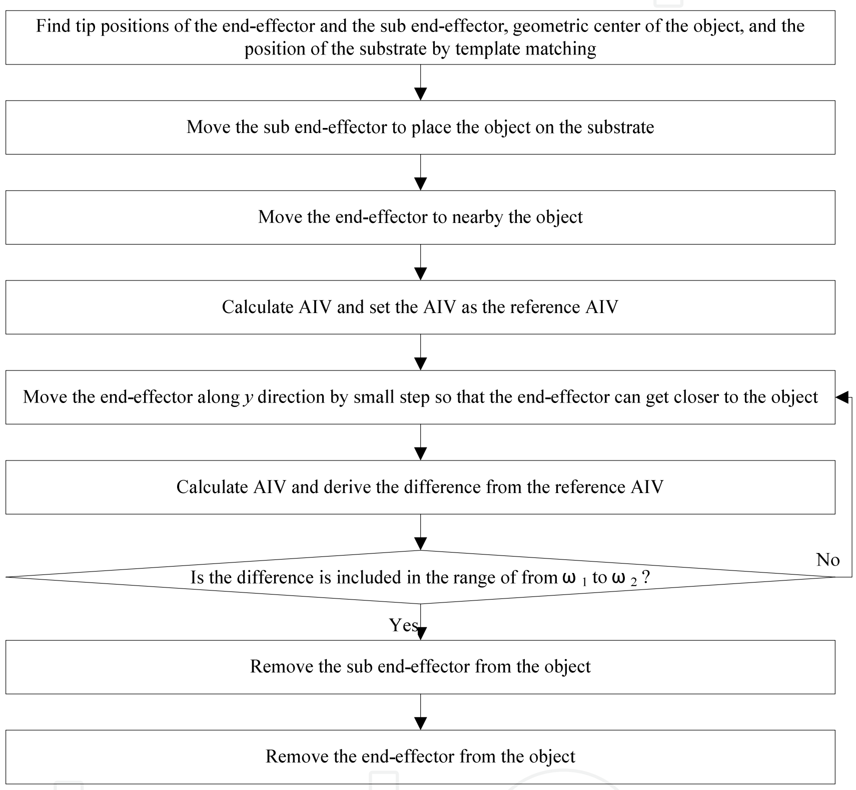

Fig. 18. Flowchart for placing operation

effector and the sub end-effector, and the geometric center of the object. The end-effector is oscillated. Using the position information, we sandwich the object between them. Next, we remove the object from the substrate by moving (controlling) the end-effector and the sub end-effector. Subsequently, we remove the end-effector from the object. In this case, the oscillation of the end-effector can reduce the adhesion force between the end-effector and the object since the oscillation in not only the bending but also the longitudinal directions of the end-effector is excited. We check the difference of AIV and judge the control of end-effector (adhesion force) is not needed, and then the checking and controlling procedures are not included in the flowchart shown in Fig. 17.
Next, we present a procedure for placing operation in Fig. 18. First, using template matching technique, we find the tip positions of the end-effector and the sub end-effector,

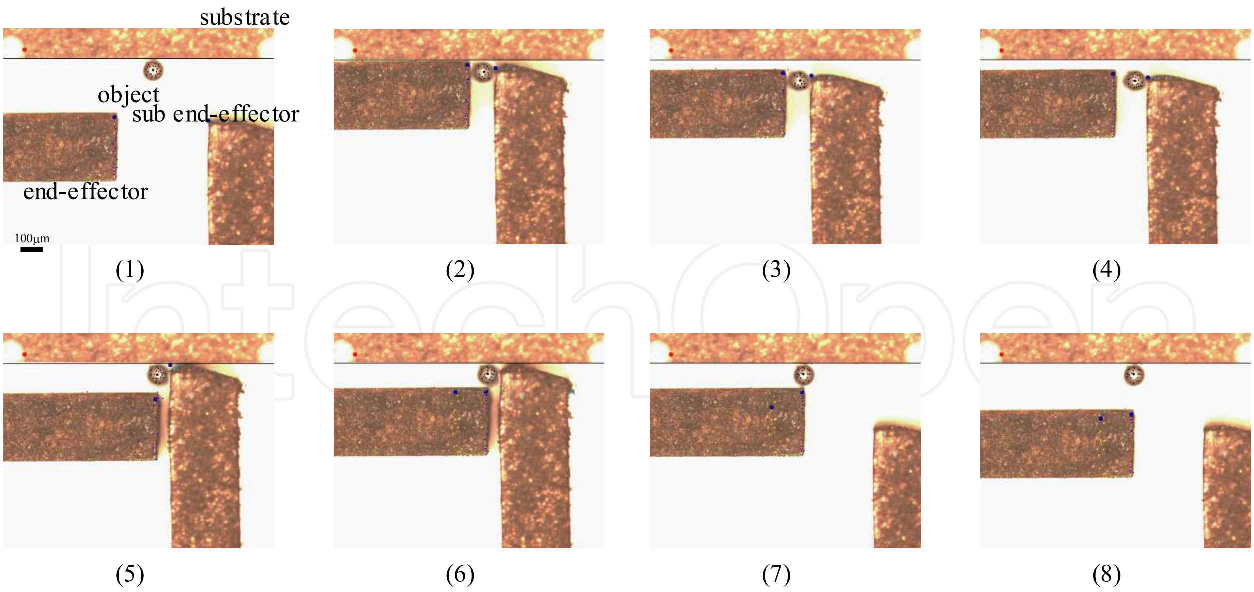

Fig. 19. Overview of the experiment for automatic micro manipulation for pick and place operation

the geometric center of the object, and the position of the substrate. Using the information, we place the object on the substrate by moving (controlling) the sub end-effector. Next, we move the end-effector to nearby the object so that the end-effector can contact with the object and push it if moving the end-effector along y positive direction (refer to y direction in Fig. 3). The end-effector is oscillated. Here, we calculate AIV and set it as the reference AIV. Next, we move the end-effector along y positive direction by small step so that the end-effector can get closer to the object. We calculate AIV and derive the difference from the reference AIV. If the difference is not included in the range of from ω_1 to ω_2, we move the end-effector along y direction by small step, and calculate AIV and the difference from the reference AIV again. If the difference is included in the range, we judge that the end-effector push the object by enough large force, reducing the adhesion force enough. In this case, we stop moving the end-effector and remove the sub end-effector from the object. Subsequently, we remove the end-effector from the object, and finish the operation.

The input voltage for PZT is square wave whose peak to peak is from 0 to 24 [V], whose duty ratio is 50[%], and whose frequency is 4th mode frequency. The threshold value ω_1 and ω_2 are, respectively, set to 5 and 10 by try and error so that the difference from the reference AIV can be detected, while the end-effector can apply enough large pushing force to the object.

The outline of the result is shown in Fig. 19. The number denotes the order of the time line. We did this operation 5 times, and all operations were successfully done. These results indicates the validity of our approach.

6. Conclusion

In this chapter, we proposed a novel method for reducing adhesion force by oscillation. By minutely oscillating the end-effector, bringing it near to an object on a substrate (table) and contacting it with the object, the adhesion force between the end-effector and the object becomes small comparing with the adhesion force between the substrate (table) and the object. Then, it is easy to remove the end-effector from the object while the object adheres to the substrate. We showed the available range of this method can be checked by checking the excitation of lower mode frequencies (than the inputted oscillation frequency), and controlled by oscillation energy. But, the method for the check is available in only limited situations due to the use of laser displacement meter: 1) The end-effector must be located at the specific point where laser displacement meter can measure oscillation; 2) the adhesion state can not be checked if something blocks the light/laser or the target leaves the measuring point. It is hard to apply this method to micro manipulation directly. Then, we developed a method to check adhesion state, using only vision information. Firstly, we developed a method to estimate the amplitude of the oscillation, using the blur resulted from the oscillation in the captured image. We call the estimated amplitude AIV (amplitude indicating value). Subsequently, we showed lower mode oscillations can be detected by AIV. Then, we developed a method for checking adhesion state (whether the adhesion force is reduced enough or not) by AIV. Based on the checking method, we developed a automatic micro manipulation system for pick and place operation. The validity of our method was shown by experiments.

7. References

Arai, F.; Andou, D. & Fukuda, T. (1996 a). Micro Manipulation Based on Physical Phenomena in Micro World (1st Report, The Reduction Method of Van Der Waals Force). *Trans. of the Japan Society of Mech. Eng., Series C*, vol.62, no.603, pp. 4286-4293.

Arai, F.; Andou, D.; Nonoda, Y. & Fukuda, T. (1996 b). Micro Manipulation Based on Physical Phenomena in Micro World(Principle and Prototype Experiments of Adhesion type Micro Endeffector). *Trans. of the Japan society of Mech. Eng., series C*, Vol.62, No.604, pp.4630-4635.

Fearing, R. S. (1995). Survey of sticking effects for micro-parts. *Proceeding of the IEEE/RSJ International Conference on Intelligent Robots and Systems*, pp. 212-217.

Haliyo, D. S.; Rollot, Y. & Regnier, (2002). S. Manipulation of micro-objects using adhesion forces and dynamical effects *Proc. of the IEEE Int. Conf. on Robotics and Automation*, pp.1949-1954.

Haliyo, D. S. & Regnier, S. (2003). Advanced applications using mad, the adhesion based dynamic micro-manipulatior. *Proc. of the IEEE/ASME Int. Conf. on Advanced Intelligent Mechatronics*, pp. 880-885.

Israelachvili, J. N. (1996) *Intermolecular and Surface Forces (Colloid Science)*, Academic Pr.

Lucas, B. D. & Kanade, T. (1981). An lterative Image Registration Technique with an Application to Stereo Vision. *Proc. 7th Int. Conf. on Artificial Intelligence*, pp.674-679.

Rollot, Y.; Regnier, S. & Guinot, J. (2002). Dynamical model for the micromanipulation by adhesion : Experimental validations for determined conditions. *J. of Micromechatronics*, Vol.1, No.4, pp.273-297.

Saito, S.; Miyazaki, H. T.; Sato, T.; Takahashi, K. & Onzawa, T. (2001). Analysis of micro-object operation based on the dynamics considering the adhesion under an sem. *Proc. of the IEEE/RSJ Int. Conf. on Intelligent Robots and Systems*, pp. 1349-1357.

Saito, S. ; Himeno, H. & Takahashi, K. (2003). Electrostatic detachment of an adhering particle from a micromanipulated probe. *J. of Applied Physics*, Vol. 93, No. 4, pp. 2219-2224.

Zesch, W. ; Brunner, M. & Weber, A. (1997). Vacuum tool for handling micro objects with a nano-robot. *Proc. of the IEEE Int. Con. on Robotics and Automation*, pp.1761-1766.

OpenCV Reference manual, Available: http://opencv.jp/opencv-1.0.0_org/docs/index.htm.

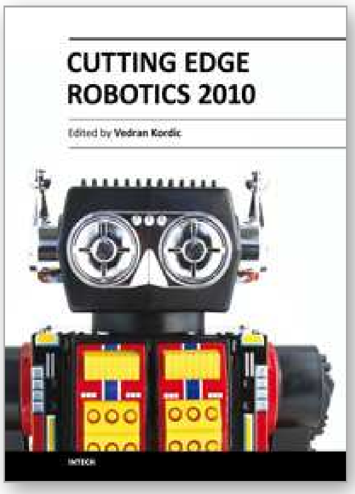

Cutting Edge Robotics 2010
Edited by Vedran Kordic

ISBN 978-953-307-062-9
Hard cover, 440 pages
Publisher InTech
Published online 01, September, 2010
Published in print edition September, 2010

Robotics research, especially mobile robotics is a young field. Its roots include many engineering and scientific disciplines from mechanical, electrical and electronics engineering to computer, cognitive and social sciences. Each of this parent fields is exciting in its own way and has its share in different books. This book is a result of inspirations and contributions from many researchers worldwide. It presents a collection of a wide range of research results in robotics scientific community. We hope you will enjoy reading the book as much as we have enjoyed bringing it together for you.

InTech Europe
University Campus STeP Ri
Slavka Krautzeka 83/A
51000 Rijeka, Croatia
Phone: +385 (51) 770 447
Fax: +385 (51) 686 166
www.intechopen.com

InTech China
Unit 405, Office Block, Hotel Equatorial Shanghai
No.65, Yan An Road (West), Shanghai, 200040, China
中国上海市延安西路65号上海国际贵都大饭店办公楼405单元
Phone: +86-21-62489820
Fax: +86-21-62489821